AUTHOR QUERIES

AUTHOR PLEASE ANSWER ALL QUERIES

PLEASE NOTE: We cannot accept new source files as corrections for your article. If possible, please annotate the PDF proof we have sent you with your corrections and upload it via the Author Gateway. Alternatively, you may send us your corrections in list format. You may also upload revised graphics via the Author Gateway.

Carefully check the page proofs (and coordinate with all authors); additional changes or updates WILL NOT be accepted after the article is published online/print in its final form. Please check author names and affiliations, funding, as well as the overall article for any errors prior to sending in your author proof corrections. Your article has been peer reviewed, accepted as final, and sent in to IEEE. No text changes have been made to the main part of the article as dictated by the editorial level of service for your publication.

AQ:1 = According to our records, Edoardo Cantù, Tiziano Fapanni, Giada Giorgi, Claudio Narduzzi, Emilio Sardini, and Mauro Serpelloni is listed as a Graduate Student Member, IEEE, Student Member, IEEE, Member, IEEE, Member, IEEE, Member, IEEE, and Senior Member, IEEE. Please verify.

AQ:2 = Please confirm or add details for any funding or financial support for the research of this article.

AQ:3 = Table I is repeated, so we have reordered the remaining tables in the sequential order and its correspondign citations. Please check.

AQ:4 = Please confirm that Ref. [34] is correct as set.

AQ:5 = Please provide the organization name, organization location, and report no. for Ref. [45].

AQ:6 = Please provide the publisher name and publisher location for Ref. [46].

Printed Multi-EMG Electrodes on the 3D Surface of an Orthosis for Rehabilitation: A Feasibility Study

Edoardo Cantù, *Graduate Student Member, IEEE*, Tiziano Fapanni, *Student Member, IEEE*, Giada Giorgi, *Member, IEEE*, Claudio Narduzzi, *Member, IEEE*, Emilio Sardini, *Member, IEEE*, Mauro Serpelloni, *Senior Member, IEEE*, and Sarah Tonello

***Abstract*—The article proposes the development of an innovative prototype of smart orthosis with a fully integrated multi-electrodes matrix for electromyography (EMG), to improve non-invasive personalized recording during rehabilitation. Both electrodes and conductive tracks were effectively printed onto the three-dimensional (3D) surface of the orthosis through Aerosol Jet Printing. Results from morphological and electrical characterization of printed elements showed an average thickness of 22.2 μm (relative standard deviation of 11%) with average resistivity of about $51 \cdot 10^{-8}\,\Omega{\cdot}$m (relative standard deviation of 10%) and an electrode-to-skin impedance comparable to the one of commercial dry electrodes. Portability and comfort were enabled by customized light-weight conditioning electronics attached to the orthosis allowing wireless data transmission. Muscular activity from three subjects was then evaluated while performing the same tasks involving multiple muscles. Results confirmed the ability of the device to monitor the activity of gastrocnemius muscle during both a sit-to-stand task and isometric contractions, both for intra- and inter-subjects' analyses. A comparison with commercial surface EMG electrodes and with literature confirmed similar features both in time and frequency. Overall, the results presented suggest the possibility to exploit the potential to print customized electrodes onto 3D surfaces to fabricate smart personalized wearable orthoses useful to capture valuable feedback to improve effectiveness, consciousness, and interactivity during daily activities and specific exercises, for both patient and medical personnel.**

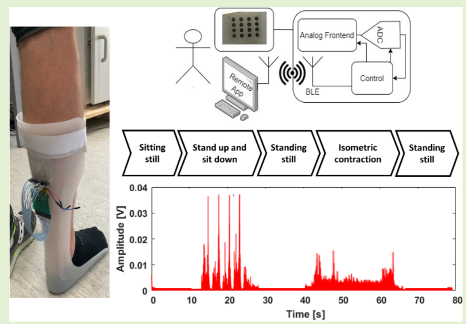

***Index Terms*—Aerosol jet printing, printed EMG electrodes, 3D printing, smart wearable devices.**

I. Introduction

THE countless advantages of wearable devices in terms of low cost, design flexibility, miniaturization and wide fields of applicability are pushing the research to investigate novel techniques to enable effective integration of sensors within smart and stand-alone devices that can improve the final users' life experience [1]–[4]. Particular effort has been addressed in the recent decade to combine wearable devices user-friendliness and low-cost with robustness, accuracy and repeatability required to improve the reliability of the data extracted from those devices [5].

Among the wide variety of parameters monitorable using wearable devices, electromyographic (EMG) signal represents a highly investigated and discussed one. The evaluation of EMG time and frequency content represents a valuable tool to provide feedback on the physio-pathological state of muscles and of its neuromuscular junction [6], to open the path to applications in the field of human-machine interfaces, but also to enable continuous monitoring of muscular progress during post-stroke recovery or rehabilitation [7], [8].

Focusing on home-based monitoring, the effective integration of EMG electrodes, of customized signal processing and transmission circuit directly onto wearable devices together is highly demanded. Currently, most of the EMG recording is still performed in laboratories using standard single-use surface electrodes following complex protocols, with the need of medical personnel to ensure proper positioning and

Manuscript received December 22, 2020; revised January 26, 2021; accepted January 29, 2021. This work was supported by the Department of Information Engineering, University of Padova, through the Networking Project "Smart WEArable Sensors for E-Health applications (SWEASE): A powerful combination of advanced printing technologies and efficient signal processing techniques." The associate editor coordinating the review of this article and approving it for publication was Prof. Rosario Morello. *(Corresponding author: Sarah Tonello.)*

Edoardo Cantù, Tiziano Fapanni, Emilio Sardini, and Mauro Serpelloni are with the Department of Information Engineering, University of Brescia, 25131 Brescia, Italy (e-mail: mauro.serpelloni@unibs.it).

Giada Giorgi, Claudio Narduzzi, and Sarah Tonello are with the Department of Information Engineering, University of Padova, 35131 Padua, Italy (e-mail: sarah.tonello@unipd.it).

Digital Object Identifier 10.1109/JSEN.2021.3059308

signal interpretation. Thus, the integration of those electrodes with orthoses or wearable devices could improve customization depending on patient characteristics and rehabilitation needs. Furthermore, relying on integrated electrodes can ensure effective long-term monitoring with higher repeatability and accuracy due to standardized positioning, improving rehabilitation outcomes without having to rely on bulky devices in hospitals or laboratories.

Of course, to enable the diffusion of home-based wearable devices for rehabilitation, many issues must still be addressed to improve user-friendliness and allow non-skilled patients to use the device ensuring accuracy, reliability and robustness, as required for commercialization in non-controlled environments (e.g. hospital, homes) [3]. Thus, finding the most suitable trade-off between cost, performances and user comfort is often non-trivial [9]. In particular, different kinds of interferences may affect the desired signal from the environment or due to possible device misplacements from non-expert users [10]. Exciting challenges are further related to data transmission towards an external application where using a stable connection to provide reliable information, and to strategies to achieve a proper signal compression and feature classification to limit dissipated power, enabling the use of miniaturized batteries and memories to limit the invasiveness for the patient [11]–[14]. Thus, an essential requirement to be effective during rehabilitative tasks is the total unobtrusiveness of the equipment used to retrieve the signals, to leave the patient free to perform all the exercises without any impairment [15].

Considering this request, one of the most pressing requirements is to develop embedded customized electrodes directly on the surfaces of wearable devices, providing a ready-to-use personalized sensing device. Currently, most of the examples of electrodes integration with wearable devices show the usage of commercial EMG surface electrodes combined with an orthosis to model knee joints [16], to design a smart mechatronic orthosis [17], [18], to enable automatic recognition of terrain characteristics through an instrumented leg orthosis [19], to assess the effect of an exoskeleton [20]. Despite relevant usefulness of EMG signal is confirmed from all the results obtained, none of the above presents a fully integrated design. Thus, adhesive electrodes positioning is still needed additionally to orthosis wearing, with possible limitations in terms of unobtrusiveness, portability and connectivity. Furthermore, those few examples of stand-alone devices provided [21], despite wireless connection is often ensured, present still bulky electrodes not fully integrated with the orthosis, non-suitable for home-based continuous monitoring since they are impairing patient movements.

In this framework, printed electronics represents a unique set of enabling technologies, in terms of process flexibility, cost reduction, miniaturization and/or improvement of the integrability of EMG and its conditioning circuit into wearable devices [5]. A wide number of different techniques, substrates and inks have been proposed in the literature to try to integrate EMG electrodes in wearable systems. Screen printing (SP), inkjet printing (IJP) and roll-to-roll (RR) [22] were employed in the production of unconventional prototypes attempting to improve flexibility and strain of EMG electrodes [23] [24]. The most promising strategies comprehend textiles [25], [26], temporary tattoo-like electrodes [4], conductive polymers like poly-3,4-ethylenedioxythiophene doped with poly(styrene sulfonate) (PEDOT:PSS) or elastomers blended with silver or carbon nanoparticles inks [1], [2], [27]–[29]. Among those, tattoo-like permanent electrodes represent the most recent highly investigated solution to improve unobtrusiveness and enhance performances both in terms of signal to noise ratio (SNR) than of stability [4]. Despite they clearly represent a promising conformable and non-invasive solution, several challenges in terms of durability and toxicity effect due to long term tattoo-skin interaction are still under investigation. Thus, since allergies and unwanted reactions due to continuous tattoo-skin interaction could affect the possibility to perform long term measurement, deep investigation of the chemistry of employable inks, of their durability and of the overall invasiveness of the technique is highly demanded. Considering those challenges, a competitive solution could be the direct integration of customized electrodes onto the 3D surfaces of orthosis or prosthesis. This can guarantee from one side conformable skin-to-electrode interaction and from the other improved stability due to a more robust ink-to-substrate interaction. Aiming to this solution, however, none of the above-mentioned techniques can serve, since they are all printing in two dimensions, limiting the integration of electrodes onto 3D surfaces of wearable devices. In this perspective, emerging printing techniques, such as Micro-Dispensing or Aerosol Jet Printing (AJP), are opening the way to the novel attractive possibility to directly embed electrodes with totally customized positions, geometries and materials onto 3D surfaces of wearables (orthosis and prosthesis) to realize a properly "smart" wearable device [30]–[32].

Considering this framework, we propose here the development of a fully embedded EMG matrix and its conditioning electronics onto the 3D surface of a rehabilitation leg orthosis using AJP. The aim is to pursue thanks to printed electronics a totally innovative approach for making "smart" an already commercially available orthosis, with a personalized approach, depending on the specific target muscles, on patient anatomy and on rehabilitation requirements. After describing the process adopted to fabricate electrodes, conductive tracks, and to integrate them with the portable conditioning electronics, an impedance-based characterization of the device and preliminary in vivo acquisitions are presented, comparing the performances with the ones from standard pre-gelled electrodes.

II. Device Fabrication and Characterization

A. Fabrication and Integration of the Electrodes With the Wearable Device

In order to set up the optimal printing and curing parameters to achieve suitable conductivity of the printed elements on the final orthosis, preliminary printing runs were performed on test samples. In detail, polypropylene (PP) samples with the same characteristics of the final orthoses in terms of material, diameter, and curvature were selected. The position of electrodes and tracks and their electrical connections were carefully designed

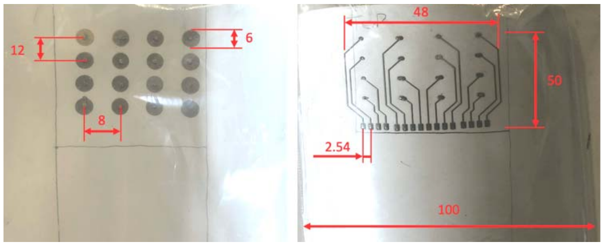

Fig. 1. Final layout of the prototypes for inner and outer features (quotes in mm).

Fig. 2. Electrodes and tracks printed on the orthosis; a tester wearing the devices with the electronics.

to minimize skin-impedance and to limit invasiveness for the end-user. EMG electrodes were printed on the center of the inner (concave) surface, while tracks with pads on the outer (convex) surface of the concave samples, replicating the positioning of the EMG matrix and the electronics in the final orthosis. A proper electrical connection between each electrode and its corresponding track was obtained by drilling 0.5 mm diameter openings on fiducial markers previously printed to evaluate the encumbrance area of the elements to be printed. Each hole was filled with conductive ink, the same material used to make the printed conductive tracks. Two consecutive depositions of silver ink were performed for tracks, pads and the first layer of each electrode, followed by two depositions of silver chloride ink only on the electrodes to ensure a better coupling with human skin.

The printed layout is shown in Figure 1, while the positioning of the electrode matrix on the inner face and of the traces on the outer face of the device can be appreciated in Figure 2. The position of the matrix was carefully set up to provide correct acquisitions of EMG signals of the gastrocnemius muscle, taking as reference the standard positioning of commercial pre-gelled Ag/AgCl electrodes during surface EMG recording of those muscles [33].

AJ 300 printer (Optomec, Albuquerque, New Mexico, USA) was the Aerosol Jet printer selected to realize our prototypes. Silver ink Metalon HPS 108-AE1 (Novacentrix, Austin, Texas, USA) is the selected conductive Ag ink to print tracks, pads and the first layer of each electrode. It is an aqueous suspension of silver flakes, specifically formulated for AJP, containing a polymeric additive to strengthen the adhesion to plastic substrates, thus avoiding the risk of detachment and improving long-term stability. Silver chloride ink (XA-3773) with Ag/AgCl weight proportion ratio of 8/2 was purchased by Fujikura Kasei. Co. Ltd. (Shibakouen Minato-ku, Tokyo, Japan) together with its thinner to realize the top layer of our electrodes. A dilution of the ink, with its specific thinner, was mandatory to obtain a proper viscosity for the printing stage (ink starting viscosity was 300±50 dPa· s), following the equations reported in the literature regarding a two-component blend [34]. The ink was deposited at 23 °C with a viscosity of about 19.5 mPa·s [35].

TABLE I
AEROSOL JET PRINTER PROCESS PARAMETERS FOR EMPLOYED INKS

	Ag	Ag/AgCl
Sheath gas flow (SCCM)	450	500
Atomizer gas flow (SCCM)	1150	1150
Exhaust gas flow (SCCM)	1060	1100
Printing speed (mm/s)	2	3.5
Plate temperature (°C)	30	50

Table I resumes the process parameters employed during the manufacturing phase. Ag deposition was followed by a one-hour-long curing step performed in an oven at 140 °C, while Ag/AgCl deposition was followed by a sintering step in the oven for 30 minutes at 125 °C. After the printing and sintering phase, corner connectors were glued to the supports in correspondence of the pads with a conductive silver epoxy (CW2400, Chemtronics) mixing the two parts in equal amounts and performing a curing step in the oven at 70°C for 20 minutes.

The board containing the conditioning electronics and the battery was attached to the outer surface of the device before the actual tests were performed. The specifications of this part will be discussed later in section II.B. A total number of three prototypes were realized. The final layout of the device can be seen in Figure 2, printed on the orthosis and worn by a tester with the complete electronics.

B. Morphological and Electrical Characterization of Printed Electrodes

A morphological test on the printed lines was performed thanks to Filmetrics Profilm 3D optical profilometer (Filmetrics Inc., 10655 Roselle St., San Diego, CA, USA), to evaluate the shape of the printed lines. It is based on state-of-the-art white light interferometry (WLI), a non-contact optical method for surface height measurements on 3-D structures, to measure surface profiles and roughness down to 0.05 μm. The instrument works in the range of 50 nm–10 mm with substrates and materials characterized by a reflectance between 0.05–100%. The system implements a 5MP camera, the Nikon CF IC Epi Plan 20x model (field-of-view: 1.0 mm x 0.85 mm). The samples were measured in three different areas along the total length to assess the uniformity of the thickness. The parameters evaluated in this phase are the total thickness, calculated as the difference between the maximum height and 1% of this value, and line width, calculated as the difference between two consecutive 1% values on the two sides of the maximum height. Results show an average line width

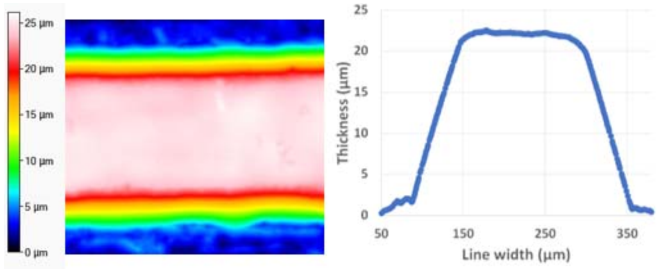

Fig. 3. Profilometer results for printed traces.

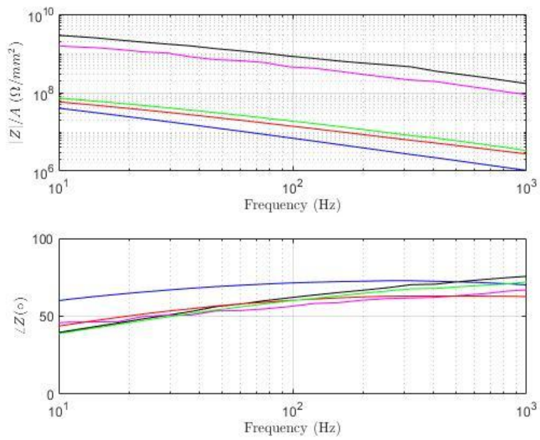

Fig. 4. Comparison of the impedances of different electrodes normalized on electrode area on subject 1. Wet commercial electrodes in blue, commercial dry electrodes with/without sweat simulation in green/black and AJ printed dry electrodes with/without sweat simulation in red/magenta.

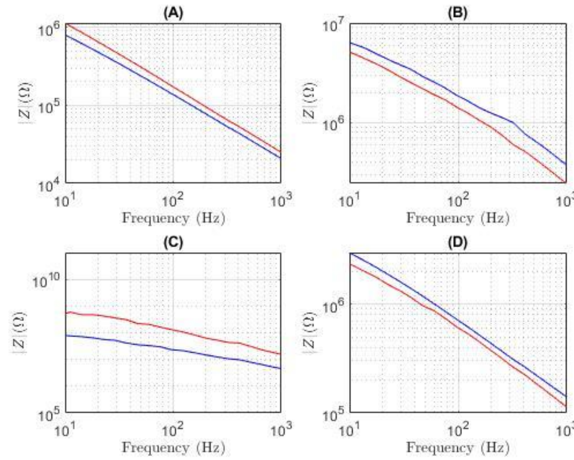

Fig. 5. Comparison of the impedances of same electrodes between the two subjects (1 in red, 2 in blue). Wet commercial electrodes (A), commercial dry electrodes without sweat simulation (B) and AJ printed dry electrodes without/with sweat simulation (C)/(D).

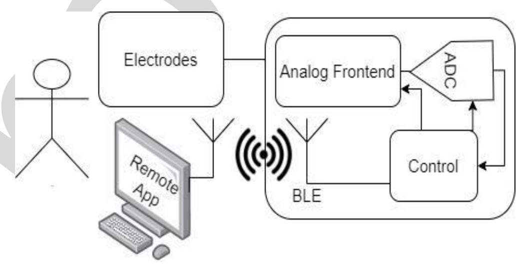

Fig. 6. Architecture of the developed wearable device.

of 320.85 μm (relative standard deviation of 10%), a total thickness of 22.2 μm (relative standard deviation of 11%) and a resistivity of 51 10^{-8} Ω m (relative standard deviation of 28%), which is in agreement with what declared by the manufacturer on the datasheet in the order of $10^{-8}\Omega$ m, with values varying depending on deposition and curing parameters. Figure 3 shows an example of the profile obtained for the printed features.

C. Device Impedance Characterization

In order to evaluate the performances of the electrodes directly embedded on the devices by means of AJP, we compared their electrode-to-skin impedance with the one of two types of commercially available surface electrodes: wet Ag/AgCl electrodes (Kendall), and dry electrodes (DRV175). For each electrode/subject combination, three measurements were acquired at rest, placing a couple of electrodes on the gastrocnemius muscle of two healthy volunteers. Only for the dry electrodes, a set of measurements with water-humid skin were acquired to simulate sweating. All the measurements were acquired with a portable impedance analyzer (Palmsens3 3EIS), configured to record impedance sweep in a range of frequencies from 10 to 1000 Hz, comprising the range of interest of EMG signal. All the measures were normalized with respect to the active area of the electrodes to provide better means of comparison. Both an intra- and an inter- subject analysis were performed.

As highlighted from Fig.4, the comparison among electrodes on the same subject showed a great similarity between our AJ printed electrodes and the commercial dry ones, with a difference around 20% for magnitude spectrum with sweat simulation and a difference of around 46% without sweat simulation. Regarding inter-subject variability, as highlighted from the average impedances for two subjects in each configuration shown in Fig. 5, comparable results could be obtained. The differences in terms of magnitude can be explained taking into consideration the variability in inter-subject device positioning, subject training and muscular anatomy.

D. Signal Acquisition Section

In the present section, we briefly discuss development choices and system architecture. During electronic device development, user comfort and technical aspects were considered as key requirements. According to these considerations, the architecture depicted in Fig. 6, was developed to provide an 8-channel front-end with integrated Bluetooth Low Energy (BLE) real-time communication using as few components as possible to reduce both the power absorption and the invasiveness of the wearable device.

We employed an ADS1298 integrated frontend for biopotential signals produced by Texas Instruments which includes an 8-channel 24-bit ADC with built-in programmable gain amplifiers and serial chip-to-chip communication. The control and communication tasks are performed by a CYBLE-222014-01

Cypress Semiconductor microcontroller whose firmware allows a configuration to perform 1 kHz signal sampling and its transmission through BLE notifications to a remote unit. The system communication was tested, and it was possible to achieve an average throughput of 27763 B/s with a percentage of correctly received packets higher than 99%. The wearable device was completed with a 1000 mAh LP603450 LiPo battery that can nominally power the system for up to 30 hours.

III. In Vivo Acquisitions

A. Protocol for EMG in Vivo Acquisition

In order to assess proper functioning, the novel device was tested on three different normal abled subjects, measuring the activity of gastrocnemius while executing specific tasks, compatible with the orthosis and that are reported in the literature as useful during rehabilitation session or routine activities [36], [37]: The protocol was then composed by the following tasks:

1) Sitting still
2) Standing and sitting tasks
3) Standing still
4) Isometric contraction of the gastrocnemius muscle
5) Standing still

The acquisition of each task was repeated three times for each subject. For each subject, a complete set of measurements performing the same tasks was also executed using standard pre-gelled commercial surface EMG electrodes, to have a reference. The analysis of the signals from both commercial and AJ printed electrodes was performed exploiting well known and established features in time, frequency and spatial, to be able to compare results from our device with other studies performed in the literature.

B. Signal Processing

Relying on widely accepted strategies reported in the literature, acquired data were processed and analyzed using MatLab to filter the interferences, recognize the contraction events and extract relevant frequency, time and spatial features.

1) Signal Denoising and Filtering: Interferences due to poor skin-electrodes contact and electromagnetic interferences are common in applications dealing with wearable electronics [10]. Raw data were then processed using a notch filter at 50Hz to remove power interferences and then using a bandpass filter between 10 and 450 Hz, to remove lower frequencies possibly due to motion artifacts or neuronal spiking, and higher frequencies due to environmental interfering signals (e.g. electromagnetic interferences). The choice of low-pass and high-pass frequencies was based on what is reported by literature, confirming that the frequency spectrum of EMG ranges from 20 to 400 Hz, with the maximum energy between 50 and 200 Hz [38], [39]. Once the raw signal was filtered, each task was isolated depending on manual timing acquired during each session. Information about both time and power of raw and filtered signals were saved as fields of a struct for each repetition.

2) Contraction Detection: The detection of each single contraction events taking place during the specific tasks was implemented relying on the use of the cumulative sum (CUSUM) of the rectified EMG signal. As reported in previous EMG analysis in the literature [41], [42], [43], this method was chosen here as an optimal trade-off in terms of low complexity and of robustness required in this application to discriminate between relax and contraction events [40]. In order to improve robustness against background noise, the traditional CUSUM method was improved, taking as a reference [44], using CUSUM-slope as a measure to estimate the signal content within a noisy background statistically.

TABLE II
TIME FEATURES SELECTED FROM LITERATURE [1], [45]

Feature	Equation
MAV	$g(j) = \frac{1}{N} \sum_{i=j-\frac{1}{2}(N-1)}^{j+\frac{1}{2}(N-1)} \lvert s(i) \rvert$
RMS	$g(j) = \sqrt{\frac{1}{N} \sum_{i=j-\frac{1}{2}(N-1)}^{j+\frac{1}{2}(N-1)} s(i)^2}$
WL	$g(j) = \sum_{i=j-\frac{1}{2}(N-1)}^{j+\frac{1}{2}(N-1)-1} \lvert s(i+1) - s(i) \rvert$
WAMP $s_{\lim} = 10$ $s_{\lim} = 20$	$g(j) = \sum_{i=j-\frac{1}{2}(N-1)}^{j+\frac{1}{2}(N-1)-1} [v(\lvert s(i+1) - s(i) \rvert)]$ $v(s) = \begin{cases} 1, & \text{if } s \geq s_{\lim} \\ 0, & \text{otherwise} \end{cases}$

Briefly, defined x_i the EMG signal the CUSUM Ci was calculated according to the (1) reported in [44].

$$C_t = \sum_{i=1}^{t} x_i - \mu C_t = \sum_{i=1}^{t} x_i - \mu \tag{1}$$

The first derivative of Ci was then calculated, and a moving average applied to avoid the identification of background random fluctuation as contraction onsets or offsets. Contraction onset and end could be then identified by comparing the first derivative with a threshold to discriminate significant changes with respect to the standard deviation of the background noise. The indexes corresponding to the contractions' onset were saved depending on the moment in which the first derivative becomes higher than the threshold, and the indexes of the end of the contraction as those moments in which the first derivative becomes lower than the threshold.

3) Time, Frequency and Spatial Features: In order to perform intra- and inter-subject comparison, a widely accepted method in the literature is the one relying on specific time features. Among the various available, we selected here four-time features (Mean Absolute Value (MAV), Root Mean Square (RMS), Wavelength (WL) and Willison Amplitude (WAMP) since they are referenced as the most relevant in the literature using EMG for rehabilitation applications were indicated as the most useful [1], [45].

Although time-features are the most frequently adopted method to characterize EMG signals and to compare different sessions, often frequency content analysis represents a useful complementary tool. During rehabilitation sessions or when evaluating the comfort of prosthesis or orthosis, one of the key aspects is to assess muscle fatigue during long or repetitive tasks. This is useful to provide feedback to the patient and to inform medical personnel about the improvement during long-term monitoring. Mean (MNF) and median (MDF) frequency (defined as detailed in equations 2 and 3) were selected as frequency features since they are indicated in the literature as most related to fatigue [46].

$$\int_0^{MDF} P(t,f)df = \int_{MDF}^{\infty} P(t,f)df = \frac{1}{2}\int_0^{\infty} P(t,f)df \quad (2)$$

$$MNF = \frac{\int_0^{\infty} f P(t,f)df}{\int_0^{\infty} P(t,f)df} \quad (3)$$

After computing the frequency spectrum of the segmented EMG during the contraction using the Short-Time Fourier transform (windows length = 128 ms, overlap = 50 ms), MNF and MDF were calculated starting from the definitions (2) and (3) as referenced in [46].

In addition to time and frequency features, since the printed matrix represents a multichannel system, spatial features were also extracted to assess the ability of the device to evaluate signal distribution during different tasks.

The content of each of the 8 channels was evaluated at discrete time points corresponding to maximum RMS amplitude, showing how the signal was traveling along with the muscle during different tasks.

4) Correlation Analysis: Correlation analyses have been performed to characterize the device both intra- and inter-subjects, adapting protocols often adopted in the literature to evaluate EMG monitoring on single or multi-users [47]–[49]. Considering each analysis performed on a single subject, cross-correlations of each channel with the others were calculated to provide a table with the maximum correlation coefficients obtained among the different channels and the lag at which they were obtained. Considering channels activation during the same task performed by different subjects, a cross-correlation between each corresponding channel was performed, to assess how the device can collect signals from different subjects with different anatomical features.

C. Results From in Vivo Acquisitions

EMG signals acquired and analyzed (as described in sections III A and B) confirmed the functionality of the dry EMG matrix embedded in the orthosis. In particular, the possibility to detect muscle activation, muscle fatigue, contraction spatial location and to monitor muscle activity from different areas of the muscle during complex tasks were demonstrated. To extensively and organically show and discuss experimental results, they will be summarized here in three specific sections, each to highlight different investigated aspects. The first one is exclusively dedicated to the comparison between data acquired from AJ printed dry electrodes with the ones from standard pre-gelled Ag AgCl electrodes that represent the commercially available gold standard for EMG analysis. The second one will evaluate on a single subject how the different channels are correlated among them during a stand up and sit down task and how it is possible with a color map to show contraction time and spatial evolution. The third one will show how the system work considering different subjects, in terms of time features, frequency features and correlation among the same channels.

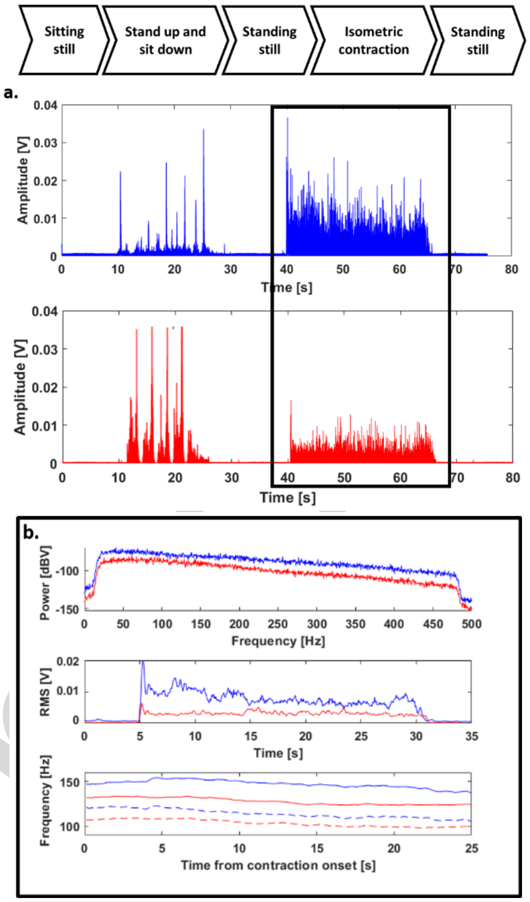

Fig. 7. a. Comparison of the full protocol acquired with reference commercial electrodes (blue) and with AJ printed electrodes (red); b. Analysis of the time and frequency features of the EMG signal acquired from a single contraction respectively with commercial (blue) and AJ printed electrodes (red).

1) Comparison Between AJ Printed Electrode Matrix and Commercial Electrodes: Results obtained from the comparison between the parameters of EMG signals measured with AJP and with commercial pre-gelled surface electrodes showed a comparable ability to follow qualitatively the different time evolution of the tasks performed. Comparable qualitative trends could be obtained both in terms of RMS amplitude than of frequency features. However, quantitative differences could be observed both in terms of RMS amplitudes, of SNR and of frequency content. In detail the SNR was computed both linearly than in dB, using the average RMS values measured during a contraction event (RMS signal) and during rest (RMS rest). RMS amplitude values of the EMG recorded using printed electrodes appeared reduced with respect to the ones obtained with commercial electrodes (Figure 7), both during rest (average reduction 40%) and during contraction (60%). The higher reduction of the RMS observed during contraction than during rest caused a reduction of the SNR associated with the printed electrodes respect to the commercial ones of nearly 5 dB (AJP electrodes showed SNR in a range between 24 to 27 dB compared to the 30 dB of the commercial surface electrodes).

Regarding frequency features, the range of mean and median frequency quantified from the spectrum of the AJP appear lower (10 Hz) than the range quantified from the spectrum of commercial electrodes during all the contraction. All those differences can be potentially explained considering the different dimensions of the electrodes and the different electrodes-to-skin impedance module (in agreement with what highlighted during the impedance characterization detailed in paragraph II.C). However, the amplitude of all the time features recorded allowed extracting the index of start and stop of contraction needed to perform the analysis both in time and in frequency. It can be observed, from the analysis of the mean and median frequency during the contraction, that a comparable trend could be recorded during 30 seconds of contraction. A range of frequency between 80 and 140 Hz could be observed in both systems, in agreement with the maximum frequency content of the EMG signal highlighted in the literature (20 and 150 Hz [38]).

2) Intra-Subject Task Analysis: The intra-subject functionality of the dry EMG matrix embedded in the orthosis was exploited to investigate the amplitude of the EMG signal recorded in each subject by each channel during the sit-to-stand-to-sit task, which involves different muscles at different timings. We used [36], [37], [50] as references about standard sit-to-stand and stand-to-sit biomechanical phases and muscle activity to perform a reliable comparison of the results obtained using embedded EMG dry AJ printed electrodes.

The time features extracted allowed to confirm that the device can discriminate the different events of stand up and sit down as discrete peaks (Figure 8), in agreement what obtained with commercial electrodes and to what reported in the literature [36], [37], [51]. Further, as highlighted by the comparison between the single graph referring to the commercial electrodes and the multiple graphs from 8 channels of the printed array, from this last it is possible to drive multiple information about the signal direction and spatial muscle activation with minimal invasiveness. Thus, a similar set of information could be obtained only by relying on 16 commercial electrodes, with a complex positioning protocol and with issues in terms of obtrusiveness for the patient. It was then possible to extract color maps that are visually showing the activation of the different muscles during the task (Figure 9). Thinking to a future interactive tool, this visual feedback could represent an interesting opportunity for the patient to have prompt information about the correctness of the task performed.

The correlation among the different channels confirmed that the highest value was obtained with an average delay of 0.03 ± 0.01 s among channels 1, 8 and 6 referring to the highest part of the muscle and among channels 5, 4 and 7 referring to the lowest part in each of the three subjects, suggesting the activation of the lowest part during rising and of the upper during descending (Figure 10).

Interestingly, the highest correlation values (>0.95) could be observed at delays in agreement with the distances between the peaks of RMS recorded on the different channels. In presence of a delay 0 and 0.2, maximum values of correlation would be observed respectively between nearby channels (e.g. among upper $1, 6, 8$ and lower $2, 4, 5, 7$). At higher delays 0.8 and 1 s, maximum levels of correlation could be

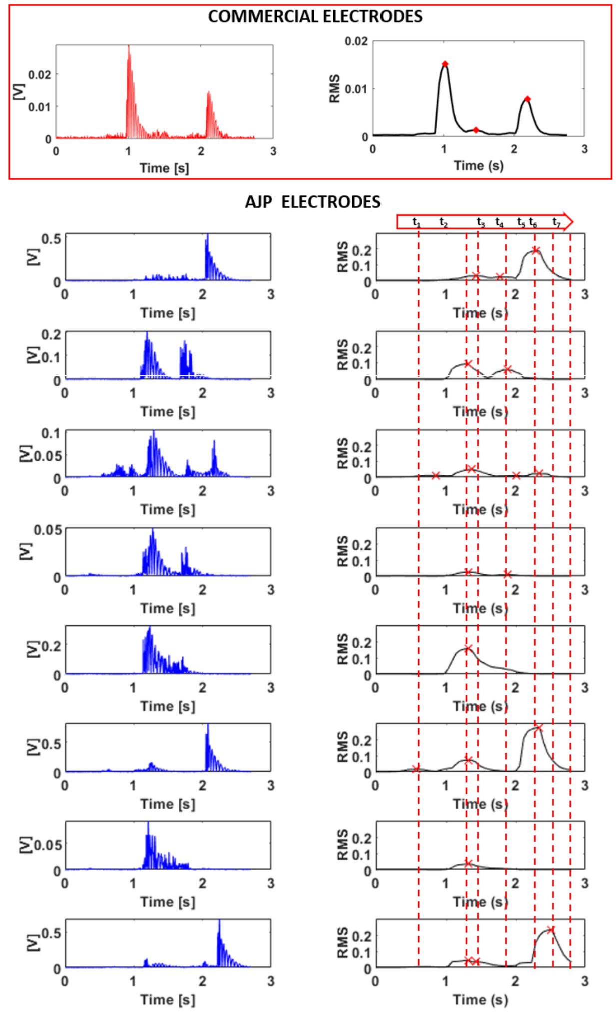

Fig. 8. From above to below channels 1 to 8 and the EMG signals recorded during a single task of sit-to-stand and stand-to-sit.

observed even between upper and lower channels. This can be comparable with the interval between rising and descending tasks, suggesting that the matrix is successfully able to detect the different timings of activation of muscle with a higher resolution than classical single-channel EMG.

Recurring peaks obtained from multiple repetitions performed using the same device (Figure 11) and from repetitions using different devices (Figure 12) suggest the proper functioning of the device even during a long-time acquisition. This gives promising results concerning the repeatability of the results obtained.

In both cases clearly, the peak of RMS EMG value due to rising and descending events could be visible. The difference in the specific shape can be explained for intra-device repetition due to imperfect contact maintained during repetition between electrodes and skin (Figure 11), while for inter-device evaluation due to a tolerance in the correct placement of the device on the muscle (Figure 12).

3) Inter-Subjects Task Analysis: Results obtained from the acquisition performed on three different subjects showed recurring time and frequency features when analyzing a single

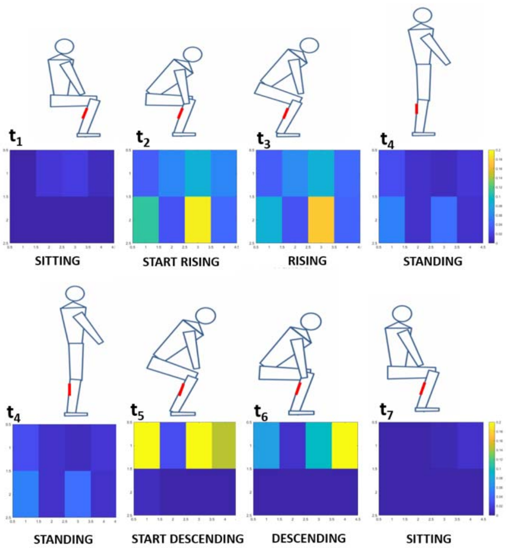

Fig. 9. Spatial features extracted during task showing the activation of each channel during the different phases.

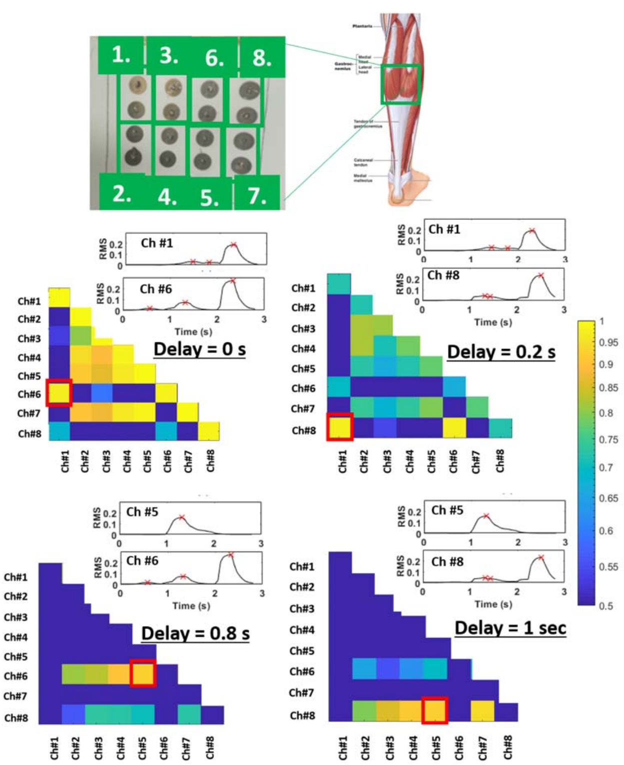

Fig. 10. Maximum correlation values among the 8 channels during sit-to-stand and stand-to-sit tasks.

contraction and a recurring pattern with two most evident local peaks when analyzing the sit-to-stand-to-sit task, in agreement with the phases of rising and descending confirmed by literature [36], [50], [51]. Despite clearly, these represent limited numbers that cannot allow stating strong assumption regarding the reproducibility, the agreement of those widely adopted features with the literature represents interesting preliminary data, is suggesting that the device is working properly on subjects with different calf dimensions (sb1:12.0 cm, sb2: 11.0 cm sb3:13.7), level of training and different sex.

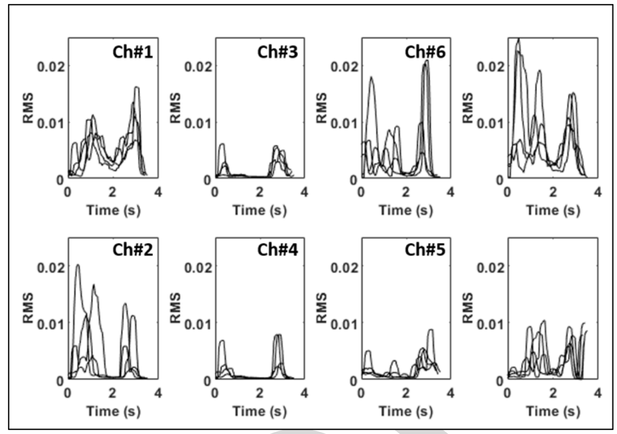

Fig. 11. RMS features obtained with multiple acquisitions of the same task on a single device.

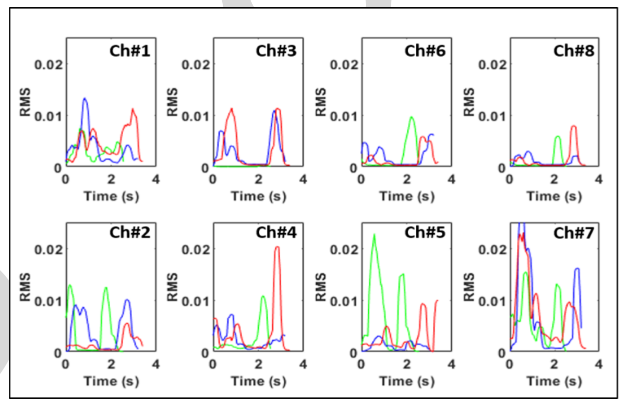

Fig. 12. RMS features obtained from the acquisition of the same task performed using three different devices on the same subject.

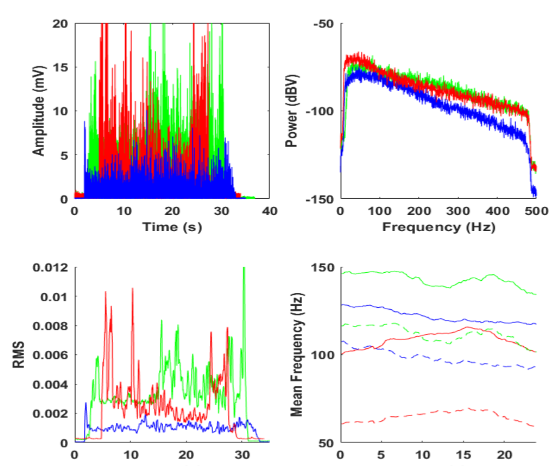

Fig. 13. Comparison of three subjects performing a single long contraction. Above filtered rectified EMG signal and its spectrum; Below: Time features and frequency features (Mean frequency solid line and median frequency dotted line).

Figure 13 and 14 report examples of comparisons among the EMG signals from the three subjects respectively during a long contraction and during a stand-up and sit-down task. Regarding the long contraction, the differences in RMS amplitude can be explained considering the variability, detailed during impedance-based characterization, due to different subject

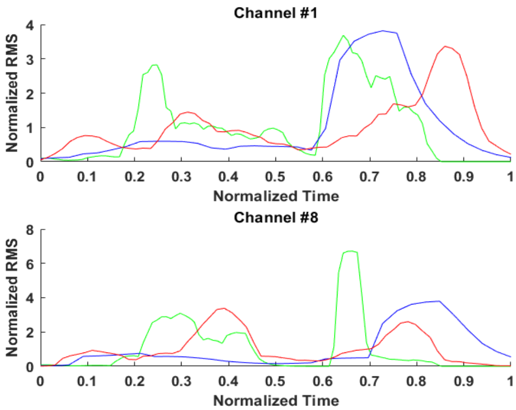

Fig. 14. Comparison among the time features calculated from the EMG of the three subjects on channels 1 and 8 while performing a sit-to-stand and a stand-to-sit task.

anatomy and variability in electrodes positioning and skin-electrodes contacts. The analysis of frequency spectrum shows comparable frequency content, with a peak located at an average frequency of 67±10 Hz, and most of the energy (70±5%) within 20 and 250 Hz, in agreement with what was reported from the literature [38], [39]. Regarding mean and median frequency, different trends can be appreciated for the three subjects, possibly due to the different levels of training bringing to different amounts and timings of muscular fibers activated during the task. Comparable ranges of mean frequencies could be observed (100−150 Hz), in agreement with the range in which the maximum EMG energy is located (70−160 Hz according to [45]) (Figure 13).

Similarly, median frequency (60−120 Hz) appears in complete agreement with results obtained with standard surface EMG electrodes [52] Interestingly, a similar decreasing trend could be observed on all the three subjects in the last 5 seconds, suggesting possibly the correlation with an ending condition of fatigue.

The comparison among the EMG recorded on the three subjects during the stand-up and sit-down task interestingly allowed to recognize comparable features in all the subjects. An example can be observed in Fig. 14 where for all the three different patients tested it was possible to detect on the same channels 1 and 8 the two peaks referring to the stand-up and sit-down task. Some differences could be observed in other channels, due to the possible tolerance in the positioning of the device and in the contact impedance in the three subjects.

IV. Conclusion

The article proposes AJP as an enabling technology for embedding a multi-EMG electrodes matrix into the 3D surface of orthosis for physiotherapy. Thanks to the advanced physics of ink deposition and curing, electrodes and tracks were directly integrated into the orthosis obtaining a resistivity in agreement with what was declared by the manufacturer and an overall geometrical variation of about 10% (line width of 320.85 μm, thickness of 22.2 μm). The device was then tested acquiring muscular activity from three subjects performing the same customized circuit, evaluating both long and short contraction and complex tasks involving multiple muscles. Results obtained in terms of recurring features with both intra- and inter-subject repetitions, in agreement with the literature, are a promising starting point for deepening in future works long term acquisitions and wider statistical analyses on multiple subjects. A comparison with the gold standard commercial electrodes for surface EMG was performed. Similar features both in frequency and time were analyzed. Due to a higher contact impedance of the electrodes, the amplitude of the time features was smaller than gelled electrodes of about 5-10 dB. Future works will try to improve this limitation by evaluating novel materials to improve the adhesion, to reduce contact impedance and to improve electrode performances. Despite this limitation, this work highlights that AJP technology could bring wearable devices to a new era, obtaining embedded sensors and conductive tracks printed directly on prostheses or orthoses. As depicted by our results, the possibility to detect contraction events, to analyze time and frequency features and to extract useful visual feedbacks for the patient with dry multiple electrodes represent a promising result to better investigate non-invasively muscular activity on larger areas, and not in a single location as in single-channel standard acquisitions. Furthermore, the extreme customizability offered by AJP opens different opportunities in terms of integration of EMG matrix with other sensors (e.g. lactate, potassium) that could provide complementary information about the fatigue and the oxygenation during physical activity. In such a way, future rehabilitation devices would be smart, not invasive for the patient and able to bring to physiotherapists or to patient valuable feedback to improve effectiveness, consciousness and interaction during daily activities and specific exercises.

References

[1] Z. Abass, W. Meng, S. Q. Xie, and Z. Zhang, "A robust, practical upper limb electromyography interface using dry 3D printed electrodes," in *Proc. IEEE/ASME Int. Conf. Adv. Intell. Mechatronics (AIM)*, Jul. 2019, pp. 453–458.

[2] Y. Hu *et al.*, "Stretchable and printable medical dry electrode arrays on textile for electrophysiological monitoring," in *Proc. IEEE 69th Electron. Compon. Technol. Conf. (ECTC)*, May 2019, pp. 243–248.

[3] D. De Venuto, S. Carrara, J. Rabaey, and J. Ohta, "Guest editorial special issue on sensors and interfaces for mobile healthcare," *IEEE Sensors J.*, vol. 16, no. 23, p. 8185, 2016.

[4] S. Shustak *et al.*, "Home monitoring of sleep with a temporary-tattoo EEG, EOG and EMG electrode array: A feasibility study.," *J. Neural Eng.*, vol. 16, no. 2, p. 26024, Apr. 2019.

[5] L. Inzelberg and Y. Hanein, "Electrophysiology meets printed electronics: The beginning of a beautiful friendship," *Frontiers Neurosci.*, vol. 12, p. 992, Jan. 2019.

[6] M. B. I. Reaz, M. S. Hussain, and F. Mohd-Yasin, "Techniques of EMG signal analysis: Detection, processing, classification and applications," *Biol. Procedures Online*, vol. 8, no. 1, pp. 11–35, Dec. 2006.

[7] M. Hakonen, H. Piitulainen, and A. Visala, "Current state of digital signal processing in myoelectric interfaces and related applications," *Biomed. Signal Process. Control*, vol. 18, pp. 334–359, Apr. 2015.

[8] B. Rodriguez-Tapia, I. Soto, D. M. Martinez, and N. C. Arballo, "Myoelectric interfaces and related applications: Current state of EMG signal processing—A systematic review," *IEEE Access*, vol. 8, pp. 7792–7805, Jan. 2020.

[9] L. R. Quitadamo *et al.*, "Support vector machines to detect physiological patterns for EEG and EMG-based human–computer interaction: A review," *J. Neural Eng.*, vol. 14, no. 1, Feb. 2017, Art. no. 011001.

[10] G. Li, Y. Li, L. Yu, and Y. Geng, "Conditioning and sampling issues of EMG signals in motion recognition of multifunctional myoelectric prostheses," *Ann. Biomed. Eng.*, vol. 39, no. 6, pp. 1779–1787, Jun. 2011.

[11] N. Rabin, M. Kahlon, S. Malayev, and A. Ratnovsky, "Classification of human hand movements based on EMG signals using nonlinear dimensionality reduction and data fusion techniques," *Expert Syst. Appl.*, vol. 149, Jul. 2020, Art. no. 113281.

[12] T. Tuncer, S. Dogan, and A. Subasi, "Surface EMG signal classification using ternary pattern and discrete wavelet transform based feature extraction for hand movement recognition," *Biomed. Signal Process. Control*, vol. 58, Apr. 2020, Art. no. 101872.

[13] A. Subasi and E. Yaman, "EMG signal classification using discrete wavelet transform and rotation forest," in *Proc. IFMBE*, vol. 73, 2020, pp. 29–35.

[14] C. J. Baby, K. J. Das, and P. Venugopal, "Design of an above knee low-cost powered prosthetic leg using electromyography and machine learning," in *Proc. Adv. Intell. Syst. Comput.*, vol. 1057, 2020, pp. 339–348.

[15] M. A. Lobo, M. L. Hall, B. Greenspan, P. Rohloff, L. A. Prosser, and B. A. Smith, "Wearables for pediatric rehabilitation: How to optimally design and use products to meet the needs of users," *Phys. Therapy*, vol. 99, no. 6, pp. 647–657, Jun. 2019.

[16] V. Musalimov *et al.*, "Modelling of the human knee joint supported by active orthosis," *Int. J. Appl. Mech. Eng.*, vol. 23, no. 1, pp. 107–120, Feb. 2018.

[17] V. T. Minh, M. Tamre, A. Safonov, V. Musalimov, P. Kovalenko, and I. Monakhov, "Design and implementation of a mechatronic elbow orthosis," *Mech. Syst. Control*, vol. 48, no. 4, pp. 231–238, 2019.

[18] F. A. Ferdiansyah, P. Prajitno, and S. K. Wijaya, "EEG-EMG based bio-robotics elbow orthotics control," *J. Phys., Conf. Ser.*, vol. 1528, no. 1, 2020, Art. no. 012033.

[19] S. Gao, Y. Wang, C. Fang, and L. Xu, "A smart terrain identification technique based on electromyography, ground reaction force, and machine learning for lower limb rehabilitation," *Appl. Sci.*, vol. 10, no. 8, p. 2638, Apr. 2020.

[20] I. Kang, P. Kunapuli, H. Hsu, and A. J. Young, "Electromyography (EMG) signal contributions in speed and slope estimation using robotic exoskeletons," in *Proc. IEEE 16th Int. Conf. Rehabil. Robot. (ICORR)*, Jun. 2019, pp. 548–553.

[21] L. M. Vaca Benitez, M. Tabie, N. Will, S. Schmidt, M. Jordan, and E. A. Kirchner, "Exoskeleton technology in rehabilitation: Towards an EMG-based orthosis system for upper limb neuromotor rehabilitation," *J. Robot.*, vol. 2013, Oct. 2013, Art. no. 610589.

[22] H. W. Tan, T. Tran, and C. K. Chua, "A review of printed passive electronic components through fully additive manufacturing methods," *Virtual Phys. Prototyping*, vol. 11, no. 4, pp. 271–288, Oct. 2016.

[23] R. G. Scalisi *et al.*, "Inkjet printed flexible electrodes for surface electromyography," *Organic Electron.*, vol. 18, pp. 89–94, Mar. 2015.

[24] G. Wolterink, R. Sanders, F. Muijzer, B.-J. van Beijnum, and G. Krijnen, "3D-printing soft sEMG sensing structures," in *Proc. IEEE Sensors*, Oct. 2017, pp. 1–3.

[25] G. M. Paul, F. Cao, R. Torah, K. Yang, S. Beeby, and J. Tudor, "A smart textile based facial EMG and EOG computer interface," *IEEE Sensors J.*, vol. 14, no. 2, pp. 393–400, Feb. 2014.

[26] R. Zhang, S. Bernhart, and O. Amft, "Diet eyeglasses: Recognising food chewing using EMG and smart eyeglasses," in *Proc. IEEE 13th Int. Conf. Wearable Implant. Body Sensor Netw. (BSN)*, Jun. 2016, pp. 7–12.

[27] P. S. Das and J.-Y. Park, "A flexible touch sensor based on conductive elastomer for biopotential monitoring applications," *Biomed. Signal Process. Control*, vol. 33, pp. 72–82, Mar. 2017.

[28] P. Bifulco *et al.*, "A stretchable, conductive rubber sensor to detect muscle contraction for prosthetic hand control," in *Proc. E-Health Bioeng. Conf. (EHB)*, Jun. 2017, pp. 173–176.

[29] D. Pani, A. Achilli, A. Spanu, A. Bonfiglio, M. Gazzoni, and A. Botter, "Validation of polymer-based screen-printed textile electrodes for surface EMG detection," *IEEE Trans. Neural Syst. Rehabil. Eng.*, vol. 27, no. 7, pp. 1370–1377, Jul. 2019.

[30] F. Al-Madani, M. Kassab, B. Z. Sonmez, and H. Solmaz, "Design and development of a low-cost force feedback 3D printed myoelectric hand prosthesis," in *Proc. 21st Nat. Biomed. Eng. Meeting (BIYOMUT)*, Nov. 2017, pp. 1–3.

[31] A. Prakash, S. Sharma, and N. Sharma, "A compact-sized surface EMG sensor for myoelectric hand prosthesis," *Biomed. Eng. Lett.*, vol. 9, no. 4, pp. 467–479, Nov. 2019.

[32] S. Liu *et al.*, "Flexible noncontact electrodes for comfortable monitoring of physiological signals," *Int. J. Adapt. Control Signal Process.*, vol. 33, no. 8, pp. 1307–1318, Aug. 2019.

[33] A. Péter *et al.*, "Comparing surface and fine-wire electromyography activity of lower leg muscles at different walking speeds," *Frontiers Physiol.*, vol. 10, p. 1283, Oct. 2019.

[34] B. Zhmud, D. Ph, and A. Prof, "Lube-Tech093-viscosityblendingequations," *Lube Mag.*, no. 121, pp. 2–5, 2014.

[35] N. G. Di Novo, E. Cantù, S. Tonello, E. Sardini, and M. Serpelloni, "Support-material-free microfluidics on an electrochemical sensors platform by aerosol jet printing," *Sensors*, vol. 19, no. 8, p. 1842, Apr. 2019.

[36] K. Kaneda, "The features of muscle activity during chair standing and sitting motion in submerged condition," *PLoS ONE*, vol. 14, no. 8, Aug. 2019, Art. no. e0220602.

[37] S. Hellmers *et al.*, "Measurement of the chair rise performance of older people based on force plates and IMUs," *Sensors*, vol. 19, no. 6, p. 1370, Mar. 2019.

[38] S. A. Go, K. Coleman-Wood, and K. R. Kaufman, "Frequency analysis of lower extremity electromyography signals for the quantitative diagnosis of dystonia," *J. Electromyogr. Kinesiol.*, vol. 24, no. 1, pp. 31–36, Feb. 2014.

[39] T. Roland, S. Amsuess, M. Russold, and W. Baumgartner, "Ultra-low-power digital filtering for insulated EMG sensing," *Sensors*, vol. 19, no. 4, p. 959, Feb. 2019.

[40] P. Regier, H. Briceño, and J. N. Boyer, "Analyzing and comparing complex environmental time series using a cumulative sums approach," *MethodsX*, vol. 6, pp. 779–787, 2019.

[41] R. S. A. Brinkworth and K. S. Türker, "A method for quantifying reflex responses from intra-muscular and surface electromyogram," *J. Neurosci. Methods*, vol. 122, no. 2, pp. 179–193, Jan. 2003.

[42] W. El Falou, J. Duchêne, D. Hewson, M. Khalil, M. Grabisch, and F. Lino, "A segmentation approach to long duration surface EMG recordings," *J. Electromyogr. Kinesiol.*, vol. 15, no. 1, pp. 111–119, Feb. 2005.

[43] W. El Falou, M. Khalil, and J. Duchêne, "Adaptive approach for change detection in EMG recordings," in *Proc. Conf. 23rd Annu. Int. Conf. IEEE Eng. Med. Biol. Soc.*, vol. 2, Oct. 2001, pp. 1875–1878.

[44] D. Tam, "A theoretical analysis of an alternative CUSUM statistic called CUSUM-slope for detecting signals from background noise in a low signal-to-noise environment," *BMC Neurosci.*, vol. 10, no. S1, p. 1, Jul. 2009.

[45] A. Strazza, F. Verdini, L. Burattini, S. Fioretti, and F. Di Nardo, "Time-frequency analysis of surface EMG signals for maximum energy localization during walking," Tech. Rep., 2018.

[46] A. Phinyomark, S. Thongpanja, H. Hu, P. Phukpattaranont, and C. Limsakul, "The usefulness of mean and median frequencies in electromyography analysis," in *Computational Intelligence in Electromyography Analysis—A Perspective on Current Applications and Future Challenges*. 2012, pp. 195–220.

[47] R. N. Khushaba, "Correlation analysis of electromyogram signals for multiuser myoelectric interfaces," *IEEE Trans. Neural Syst. Rehabil. Eng.*, vol. 22, no. 4, pp. 745–755, Jul. 2014.

[48] K. Watanabe, M. Kouzaki, M. Ogawa, H. Akima, and T. Moritani, "Relationships between muscle strength and multi-channel surface EMG parameters in eighty-eight elderly," *Eur. Rev. Aging Phys. Activity*, vol. 15, no. 1, Apr. 2018.

[49] N. Malesevic *et al.*, "A database of multi-channel intramuscular electromyogram signals during isometric hand muscles contractions," *Sci. Data*, vol. 7, no. 1, p. 10, Dec. 2020.

[50] P. J. Millington, B. M. Myklebust, and G. M. Shambes, "Biomechanical analysis of the sit-to-stand motion in elderly persons," *Arch. Phys. Med. Rehabil.*, vol. 73, no. 7, pp. 609–617, Jul. 1992.

[51] A. I. Cuesta-Vargas and M. González-Sánchez, "Differences in muscle activation patterns during sit to stand task among subjects with and without intellectual disability," *Biomed Res. Int.*, vol. 2013, Jan. 2013, Art. no. 173148.

[52] C. Candotti, J. Loss, M. La Torre, M. Melo, L. Araújo, and V. Marcks, "Use of electromyography to assess pain in the upper trapezius and lower back muscles within a fatigue protocol," *Brazilian J. Phys. Therapy*, vol. 13, no. 2, pp. 144–151, Apr. 2009.

Edoardo Cantù (Graduate Student Member, IEEE) received the M.Sc. degree in mechanical engineering – biomechanics curriculum from the University of Brescia in February 2018, where he is currently pursuing the Ph.D. degree in technology for health. He has been a Researcher with a research grant with the Department of Information Engineering, University of Brescia, for seven months. His research interest includes the realization and test of sensors through additive manufacturing techniques, such as aerosol jet printing.

Tiziano Fapanni (Student Member, IEEE) received the M.Sc. *(cum laude)* degree in electronic engineering from the University of Brescia in 2019 and the Ph.D. degree in technology for health from the Department of Information Engineering. His research interests include with the development of sensors and conditioning circuit for e-skin application to monitor physiological and biochemical signals.

Giada Giorgi (Member, IEEE) received the Laurea degree in telecommunications engineering and the Ph.D. degree in microelectronics and telecommunications engineering from the University of Padova, Italy, in 2003 and 2007, respectively. She is currently an Associate Professor with the Department of Information Engineering, University of Padova. Her current research interests include distributed measurement systems and they include the development of measurement applications for wireless sensor and actuator networks (WSAN) and wireless body sensor networks (WBN).

Claudio Narduzzi (Member, IEEE) received the Laurea degree in electronics engineering from the University of Padova, Italy, in 1982. He is currently a Full Professor of Instrumentation and Measurement with the Engineering School, University of Padova. His current research interests include digital signal processing applications in measurement and distributed test and measurement systems, spectral analysis, inverse filtering, networked measurement systems, the application of advances signal processing methods, and compressive sampling.

Emilio Sardini (Member, IEEE) received the M.Sc. degree in electronics engineering from the Politecnico di Milano, Milan, Italy, in 1983. He has been a member of the Academic Senate, Board of Directors, University of Brescia, also the Deputy Dean of the Engineering Faculty, also the Director of the Department of Information Engineering, and also a Coordinator of the "Technology for Health" Ph.D. program. He is currently a Full Professor with the Department of Information Engineering, University of Brescia. His research interests include electronic instrumentation, sensors and signal conditioning electronics, and the development of autonomous sensors for biomedical applications.

Mauro Serpelloni (Senior Member, IEEE) received the M.S. *(cum laude)* degree in industrial management engineering and the Ph.D. degree in electronic instrumentation from the University of Brescia in 2003 and 2007, respectively. He is currently an Associate Professor with the Department of Information Engineering, University of Brescia. His current research interests include biomechatronic systems, contactless transmission, and signal processing for microelectromechanical systems.

Sarah Tonello received the M.S. *(cum laude)* degrees in biomedical engineering from University of Florida and also from the Politecnico di Milano in 2014, as part of the dual degree program Atlantis CRISP, and the Ph.D. degree in technology for health from the University of Brescia in 2017. She is currently a Researcher with the Department of Information Engineering, University of Padova. Her research interests include printed sensors, electronic devices, and electrochemical sensors.